CHAPTER-03

VIBRATION ANALYSIS OF TRANSVERSELY ISOTROPIC ELECTRO-MAGNETO GENERALIZED THERMOELASTIC SPHERE WITH VOIDS AND DUAL-PHASE-LAG EFFECT

3.1 Introduction

The solid voids theory with elastic materials is extended from classical theory of elasticity. The voids theory is the distribution of pores in elastic materials comprised in kinetic variables and considered as there is no significance of energetic or mechanical properties.

Herein, the main aim of the current chapter is to present dual-phase-lag (DPL) model of transversely isotropic generalized electro-magneto nonlocal thermoelastic hollow sphere/disk with voids material. The time harmonic variations have been employed to constitutive relations and governing equations. The elimination method has been employed to find field functions to present analytical results and numerical Iteration method has been applied to assumed boundary conditions. To check the effects of DPL model and nonlocal elasticity, the analytical results for frequencies and thermoelastic damping in absence/presence of magnetic field, have been represented graphically.

3.2 The governing fundamental equations and mathematical model

Here an electro-magneto transversely isotropic nonlocal elastic sphere with voids material has been presented in the context of dual-phase-lag (DPL) model of generalized thermoelasticity. The inner and outer radii of hollow sphere/disk has been assumed as $R_I = a$, $R_O = \eta a$ with domain $a \le r \le \eta a$. The problem is considered to be free from internal and external mechanical/thermal loads and free from voids volume fraction shown in Fig. 3.1. The spherical polar coordinates (r, θ, ϕ) are assumed in such a way that the field components, i.e. $\boldsymbol{u} = (u_r, u_\theta, u_\phi) = (u(r, t), 0, 0)$ is displacement vector, the equilibrated voids volume fraction and temperature component are $\varphi = \varphi(r,t)$ and $T = T(r,t)$.

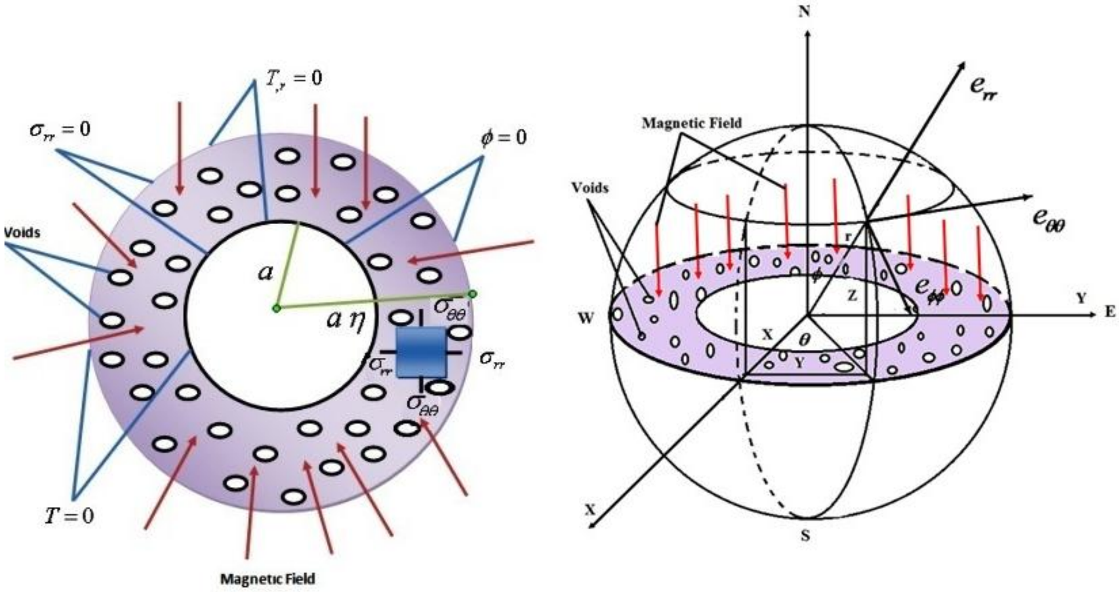

Figure 3.1: Geometry of the problem

The coordinated system has been assumed in such a way that the strength of magnetic field $\boldsymbol{H}$ proceeds in the direction of longitude of the sphere. The Maxwell's equations, generalized Ohm's law in the continua of deformation in the absence of charge density and displacement current is

$$\nabla \times \boldsymbol{E} = -\frac{\partial \boldsymbol{B}}{\partial t}, \quad \nabla \times \boldsymbol{H} = \boldsymbol{J}, \quad \boldsymbol{B} = \mu_e \boldsymbol{H}, \quad \nabla . \boldsymbol{B} = 0, \quad \boldsymbol{J} = \sigma\left(\boldsymbol{E} + \frac{\partial u}{\partial t} \times \boldsymbol{B}\right). \qquad (3.1)$$

Here the strength of magnetic field, $\boldsymbol{H} = \boldsymbol{H}_0 + h$, where, $\boldsymbol{H}_0 = (0,0,H_0)$, h is perturbation of magnetic field which is too minute that their derivatives and the product of u and h might be neglected due to linearization of equations, $\boldsymbol{B}$ is magnetic field, due to small effect of temperature gradient current density $\boldsymbol{J}$ is neglected and $\boldsymbol{E}$ is electric field. Therefore the governing equation of motion under the impact of electromagnetic field, consecutive relations, equation of voids volume fraction and heat conduction equation without body forces, heat sources and voids concentration are given by Cowin and Nanziato (1983) and Dhaliwal and Singh (1980) as:

$$\frac{\partial \sigma_{rr}}{\partial r} + \frac{(2\sigma_{rr} - \sigma_{\theta\theta} - \sigma_{\phi\phi})}{r} + F_r = \rho(1-\zeta^2\nabla^2)\frac{\partial^2 u}{\partial t^2}, \qquad (3.2)$$

$$\left(-\xi_1-\xi_2\frac{\partial}{\partial t}\right)\varphi+\alpha\nabla^2\varphi-be+MT=\rho\chi(1-\zeta^2\nabla^2)\frac{\partial^2\varphi}{\partial t^2}, \tag{3.3}$$

$$\begin{aligned}&\frac{\partial}{\partial t}\left(1+t_q\frac{\partial}{\partial t}+\frac{t_q^2}{2}\frac{\partial^2}{\partial t^2}\right)\left(\rho c_e T+T_0(\beta_r e_{rr}+\beta_\theta 2e_{\theta\theta})+MT_0\varphi\right)\\&=\left(1+t_p\frac{\partial}{\partial t}\right)\left[\frac{1}{r^2}\frac{\partial}{\partial r}\left(K_\theta r^2\frac{\partial T}{\partial r}\right)\right]\end{aligned} \tag{3.4}$$

Stress-strain-temperature relations

$$\left.\begin{aligned}(1-\zeta^2\nabla^2)\sigma_{rr}=\sigma_{rr}^L=c_{11}e_{rr}+2c_{12}e_{\theta\theta}+b\varphi-\beta_r T\\(1-\zeta^2\nabla^2)\sigma_{\theta\theta}=\sigma_{\theta\theta}^L=c_{12}e_{rr}+(c_{11}+c_{12})e_{\theta\theta}+b\varphi-\beta_\theta T\end{aligned}\right\}. \tag{3.5}$$

Strain- displacement relations

$$e_{\theta\theta}=e_{\phi\phi}=\frac{u}{r},\ e_{rr}=\frac{\partial u}{\partial r},\ e_{r\theta}=e_{r\phi}=e_{\theta\phi}=0. \tag{3.6}$$

where $(1-\zeta^2\nabla^2)\sigma_{ij}=\sigma_{ij}^L,(i,j=r,\theta)$ local-nonlocal stress relations, where the term "L" denotes local elastic medium. Here $\zeta=e_0a_0$ is a nonlocal constant parameter, where e_0 is material constant and a_0 is internal characteristic length, e_{ij}, σ_{ij}; $(i,j=r,\theta,\phi)$ are strain and stress components; $\boldsymbol{u}=(u(r,t),0,0)$ is displacement vector. T has been assumed as increase in temperature over reference temperature T_0, $\beta_{ij};(i,j=r,\theta)$ is thermal modulii, where $\beta_r=\beta_\theta=(c_{11}+c_{12})\alpha_1+c_{13}\alpha_3$; $\alpha_1=\alpha_3=\alpha_T$ is coefficient of linear thermal expansion (Dhaliwal and Singh (1980)). Here $\boldsymbol{F}_i;i=(r,\theta,\phi)$ is body force i.e. Lorentz force $\boldsymbol{F}=(\boldsymbol{J}\times\boldsymbol{B})$ in radial direction, α and b are the void parameters, ρ is mass density, χ is the equilibrated inertia, ξ_1,ξ_2 are the material constants due to presence of voids and M is thermo-void coupling parameter. The parameter K_θ is thermal conductivity, the constants t_q and t_p have been represented as the phase-lags of heat flux and temperature gradient respectively which satisfy the inequality $t_p\ge t_q\ge 0$, C_e be specific heat at constant strain, the parameters $c_{ij};i,j=1,2$ are elastic constants for transversely isotropic material whose values are given below:

$$c_{11} = \frac{E(1-\nu)}{(1+\nu)(1-2\nu)} \ , \ c_{12} = \frac{E\nu}{(1+\nu)(1-2\nu)},$$

where E is Young's modulus and ν is Poisson ratio.

Also $e = \frac{\partial u}{\partial r} + \frac{2u}{r}$ is dilatation, $\nabla^2 = \frac{\partial^2}{\partial r^2} + \frac{2}{r}\frac{\partial}{\partial r}$ is Laplace operator.

3.3 Boundary conditions

The initial conditions for nonlocal transversely isotropic hollow sphere with voids material has been considered as

$$\frac{\partial T(r,0)}{\partial t} = \frac{\partial u(r,0)}{\partial t} = \frac{\partial \varphi(r,0)}{\partial t} = 0 = T(r,0) = u(r,0) = \varphi(r,0) \quad \text{at } r = a, \eta a .$$

(3.7)

Since the domain of hollow sphere is $a \le r \le \eta a$, hence thermally insulated/isothermal traction free boundary conditions are:

Set I: $\sigma_{rr} = 0, \varphi = 0, T,_r = 0$; $\quad r = a, \quad \eta a$. (3.8)

Set II: $\sigma_{rr} = 0, \varphi = 0, T = 0$; $\quad r = a, \quad \eta a$. (3.9)

3.4 Solution of mathematical model

The Maxwell's equations (3.1) has been divided into three parts,

The first part determines as:

$$\frac{\partial H_r}{\partial t} = 0 \ , \quad \frac{\partial H_\theta}{\partial t} = \frac{1}{\mu_e}\frac{\partial E_\phi}{\partial r} \ , \quad \frac{\partial H_\phi}{\partial t} = -\frac{1}{\mu_e}\frac{\partial}{\partial r}(rE_\theta) \ , \tag{3.10}$$

The second part as

$$J_r = 0 \ , \quad J_\theta = -\frac{\partial H_\phi}{\partial r} \ , \quad J_\phi = \frac{1}{r^2}\frac{\partial}{\partial r}(r^2 H_\theta) \ , \tag{3.11}$$

where $\boldsymbol{H} = (H_r, H_\theta, H_\phi)$, $\boldsymbol{E} = (E_r, \mathrm{E}_\theta, \mathrm{E}_\phi)$ and $\boldsymbol{J} = (J_r, J_\theta, J_\phi)$.

The third part of equation (3.1) implies that there is no perturbed field applied initially in radial direction i.e. $\frac{\partial h_r}{\partial r} = 0$,which implies that $h_r = 0$. The modified Ohm's law in equation (3.1) yields:

$$J_r = \sigma E_r \ , \quad J_\theta = \sigma\left(E_\theta - \mu_e H_\phi \frac{\partial u}{\partial t} \right) \ , \quad J_\phi = \sigma\left(E_\phi - \mu_e H_\theta \frac{\partial u}{\partial t} \right). \tag{3.12}$$

It has been noticed from equations (3.10) and (3.12) that as $J_r = 0$, which implies that $E_r = 0$. The perturbation of magnetic field h is very small in comparison with strong initial magnetic field H_0 in setting the term $\boldsymbol{H} = H_0 + h$. Therefore, in eliminating J_r, J_θ, J_ϕ and utilizing equations (3.1) and (3.11) - (3.12), we obtain

$$\left.\begin{aligned} \frac{\partial H_\theta}{\partial t} &= (\sigma\mu_e)^{-1} \frac{\partial}{\partial r}\left(\frac{\partial h_\theta}{\partial r} + \frac{2h_\theta}{r} \right) \\ \frac{\partial H_\phi}{\partial t} &= (\sigma\mu_e)^{-1} \left(\frac{2}{r}\frac{\partial h_\phi}{\partial r} + \frac{\partial^2 h_\phi}{\partial r^2} \right) - H_0 \frac{\partial}{\partial t}\left(\frac{\partial u}{\partial r} + 2\frac{u}{r} \right) \end{aligned}\right\}. \tag{3.13}$$

Here $(\sigma\mu_e)^{-1}$ is magnetic viscosity. The second part of equation (3.13) yields $h_\phi = -H_0\left(\frac{2u}{r} + \frac{\partial u}{\partial r} \right)$ due to perfect electrical conductor, the magnetic viscosity $(1/\sigma\mu_e) \to 0$ as $\sigma \to \infty$, hence there is no perturbation at ∞. Therefore, the equation of motion (3.2) reduces to

$$\frac{\partial \sigma_{rr}}{\partial r} + \frac{(2\sigma_{rr} - \sigma_{\theta\theta} - \sigma_{\phi\phi})}{r} - \rho(1-\zeta^2\nabla^2)\frac{\partial^2 u}{\partial t^2} + \mu_e H_0^2 \frac{\partial}{\partial r}\left(\frac{\partial u}{\partial r} + \frac{2u}{r} \right) = 0. \tag{3.14}$$

Substituting the constitutive relations from equation (3.5) in equation (3.14) we obtain

$$\left(1 + \frac{\mu_e H_0^2}{c_{11}} \right)\left(\frac{\partial^2 u}{\partial r^2} + \frac{2}{r}\frac{\partial u}{\partial r} - \frac{2u}{r^2} \right) - \frac{\rho}{c_{11}}(1-\zeta^2\nabla^2)\frac{\partial^2 u}{\partial t^2} + \frac{b}{c_{11}}\frac{\partial \varphi}{\partial r} - \frac{\beta_r}{c_{11}}\frac{\partial T}{\partial r} = 0. \tag{3.15}$$

Applying divergence both sides to equation (3.15) we get,

$$R_h \nabla^2 e - \frac{\rho}{c_{11}}(1-\zeta^2\nabla^2)\frac{\partial^2 e}{\partial t^2} + \frac{b}{c_{11}}\nabla^2\varphi - \frac{\beta_r}{c_{11}}\nabla^2 T = 0, \tag{3.16}$$

where $R_h = 1 + \frac{\mu_e H_0^2}{c_{11}}$, $e = \frac{\partial u}{\partial r} + \frac{2u}{r}$.

To remove complexity of equations we commence the non dimensional quantities as follows

$$\left.\begin{aligned}&(U,x,\zeta_0)=\frac{1}{a}(u,r,\zeta),(\tau,\tau_p,\tau_q)=\frac{c}{a}(t,t_p,t_q),(\tau_{xx},\tau_{\theta\theta})=\frac{1}{c_{11}}(\sigma_{rr},\sigma_{\theta\theta}),\\&\theta=\frac{T}{T_0},c_0=\frac{c_{12}}{c_{11}},c=\sqrt{\frac{c_{11}}{\rho}},\phi=\frac{\chi\Omega^{*2}}{a^2}\varphi,\bar{\xi}=\frac{c}{a}\frac{\xi_2}{\xi_1},\bar{\beta}_R=\frac{\beta_r T_0}{c_{11}},\\&\bar{\beta}_\theta=\frac{\beta_\theta T_0}{c_{11}},\bar{b}^*=\frac{a^2\bar{b}}{\chi\Omega^{*2}},\bar{b}=\frac{b}{c_{11}}\end{aligned}\right\}. \quad (3.17)$$

Plugging non-dimensional quantities from proposed equation (3.17) in equations (3.3–3.5) and (3.16), we obtained following equations in non dimensional form as

$$\left.\begin{aligned}&\tau_{xx}=e+2(c_0-1)\frac{U}{x}+\bar{b}^*\phi-\bar{\beta}_R\theta\\&\tau_{\theta\theta}=c_0e+(1-c_0)\frac{U}{x}+\bar{b}^*\phi-\bar{\beta}_\theta\theta\end{aligned}\right\}, \quad (3.18)$$

$$R_h\nabla_x^2e+\bar{b}^*\nabla_x^2\phi-\bar{\beta}_R\nabla_x^2\theta=(1-\zeta_0^2\nabla_x^2)\frac{\partial^2e}{\partial\tau^2}, \quad (3.19)$$

$$\nabla_x^2\phi-a_1\left(1+\bar{\xi}\frac{\partial}{\partial\tau}\right)\phi-a_2e+a_3\theta=(1-\zeta_0^2\nabla_x^2)\frac{1}{\delta_1^2}\frac{\partial^2\phi}{\partial\tau^2}, \quad (3.20)$$

$$\left(\frac{\partial}{\partial\tau}+\tau_q\frac{\partial^2}{\partial\tau^2}+\frac{\tau_q^2}{2}\frac{\partial^3}{\partial\tau^3}\right)(\Omega^*\theta+a_4e+a_5\phi)=\left(1+\tau_p\frac{\partial}{\partial\tau}\right)\nabla_x^2\theta, \quad (3.21)$$

where $a_1=\dfrac{\xi_1a^2}{\alpha}$, $a_2=\dfrac{b\chi\Omega^{*2}}{\alpha}$, $a_3=\dfrac{M\chi\Omega^{*2}T_0}{\alpha}$, $a_4=\dfrac{\varepsilon_T\Omega^*}{\bar{\beta}_R}$, $a_5=\dfrac{cMa^3}{K\chi\Omega^{*2}}$,

$$\omega^*=\frac{c_{11}C_e}{K_\theta},\ \Omega^*=\frac{a\omega^*}{c},\ \varepsilon_T=\frac{T_0\beta_r^2}{\rho C_ec_{11}},\ \delta_1^2=\frac{\alpha}{\chi c_{11}},\ e=\frac{1}{x^2}\frac{\partial}{\partial x}(x^2U),\ \nabla_x^2=\frac{1}{x^2}\frac{\partial}{\partial x}\left(x^2\frac{\partial}{\partial x}\right).$$

We introduce time harmonic vibrations as already proposed by Pierce (1981), we have

$$\left(\bar{e},\ \bar{\phi},\ \bar{\theta}\right)=\left(e,\ \phi,\ \theta\right)e^{i\Omega\tau}, \quad (3.22)$$

where $\Omega=\dfrac{\omega a}{c}$ is the circular frequency.

Using time harmonic vibrations from equation (3.22) in equations (3.18–3.21) we get

$$\begin{pmatrix}\tau_{xx}\\ \tau_{\theta\theta}\end{pmatrix}=\begin{pmatrix}1 & 2\left(\dfrac{c_0-1}{x}\right) & \bar{b}^* & -\bar{\beta}_R\\ c_0 & \left(\dfrac{1-c_0}{x}\right) & \bar{b}^* & -\bar{\beta}_\theta\end{pmatrix}\begin{pmatrix}\bar{e}\\ \bar{U}\\ \bar{\phi}\\ \bar{\theta}\end{pmatrix}, \tag{3.23}$$

$$\begin{pmatrix}(\nabla_x^2+b_{11}) & b_{12}\nabla_x^2 & -b_{13}\nabla_x^2\\ -b_{21} & (\nabla_x^2+b_{22}) & b_{23}\\ b_{31} & b_{32} & (\nabla_x^2+b_{33})\end{pmatrix}\begin{pmatrix}\bar{e}\\ \bar{\phi}\\ \bar{\theta}\end{pmatrix}=\begin{pmatrix}0\\0\\0\end{pmatrix}, \tag{3.24}$$

where $b_{11}=\dfrac{\Omega^2}{R_h-\zeta_0^2\Omega^2}, b_{12}=\dfrac{\bar{b}^*}{R_h-\zeta_0^2\Omega^2}, b_{13}=\dfrac{\bar{\beta}_R}{R_h-\zeta_0^2\Omega^2},\ b_{21}=\dfrac{a_2}{a_1^*},\ \ b_{22}=\dfrac{a_2^*}{a_1^*},$

$b_{23}=\dfrac{a_3}{a_1^*},\ a_1^*=\dfrac{\delta_1^2-\zeta_0^2\Omega^2}{\delta_1^2},\ a_2^*=\dfrac{a_1 i\Omega\bar{\xi}^*\delta_1^2+\Omega^2}{\delta_1^2},\ b_{31}=\dfrac{\Omega^3\Omega^*\tau_q^*}{a_3^*},\ b_{32}=\dfrac{\Omega^3\tau_q^* a_4}{a_3^*},$

$b_{33}=\dfrac{\Omega^3\tau_q^* a_5}{a_3^*},\ a_3^*=i\Omega\tau_p^*,\ \tau_q^*=i\Omega^{-2}-\Omega^{-1}\tau_q-i(\tau_q^2/2),\ \tau_p^*=i\Omega^{-1}-\tau_p\ ,\ \bar{\xi}^*=i\Omega^{-1}-\bar{\xi}\ .$

In order to eliminate the parameters $\bar{e},\ \bar{\phi}\ ,\bar{\theta}$ a characteristic equation has been obtained from the non-trivial solution of equation (3.24) as

$$(\nabla_x^6-L\nabla_x^4+M\nabla_x^2-N)(\bar{e}\ ,\bar{\phi},\ \bar{\theta})=0, \tag{3.25}$$

where $L=(-b_{11}-b_{22}-b_{33}-b_{12}b_{21}-b_{13}b_{31}),\qquad N=b_{11}(b_{23}b_{32}-b_{22}b_{33})$

$M=(b_{22}b_{33}-b_{23}b_{32}+b_{11}b_{33}+b_{11}b_{22}+b_{12}b_{21}b_{33}+b_{12}b_{23}b_{31}+b_{13}b_{21}b_{32}+b_{13}b_{31}b_{22})$.

It has been investigated from characteristic equation (3.25) that it has bounded solution for $x\to\infty$, for this there is a requirement of $\mathrm{Re}(k_i)\geq 0,\ \forall\ i=1,2,3)$. Therefore roots $k_i;\ i=1,2,3$ of equation (3.25) have been achieved as given below:

$$k_1=\sqrt{\frac{1}{3}\left(2p_1\sin p_2+L\right)},\ k_2=\sqrt{\frac{1}{3}\left(L-p_1(\sqrt{3}\cos p_2+\sin p_2)\right)},\ k_3=\sqrt{\frac{1}{3}\left(L+p_1(\sqrt{3}\cos p_2-\sin p_2)\right)}$$

,

where, $p_1=\sqrt{L^2-3M},\ p_3=-\dfrac{2L^3-9LM+27N}{2L^{*3}},\ p_2=\dfrac{1}{3}\sin^{-1}(p_3)$.

Hence, the solution of equation (3.25) is obtained as

$$\overline{\theta} = x^{-\frac{1}{2}} \sum_{i=1}^{3} \left[P_i J_{1/2}(k_i x) + Q_i Y_{1/2}(k_i x) \right], \tag{3.26}$$

$$\overline{e} = x^{-\frac{1}{2}} \sum_{i=1}^{3} R_i \left[P_i J_{1/2}(k_i x) + Q_i Y_{1/2}(k_i x) \right], \tag{3.27}$$

$$\overline{\phi} = x^{-\frac{1}{2}} \sum_{i=1}^{3} S_i \left[P_i J_{1/2}(k_i x) + Q_i Y_{1/2}(k_i x) \right], \tag{3.28}$$

where $R_i = \dfrac{k_i^2 (b_{13} b_{21} - b_{23}) - b_{11} b_{23}}{k_i^4 b_{13} + (b_{13} b_{22} + b_{12} b_{23}) k_i^2}$, $\quad S_i = \dfrac{k_i^2 b_{31} + b_{22} b_{31} - b_{21} b_{32}}{k_i^4 + (b_{22} + b_{33}) k_i^2 + b_{22} b_{33} - b_{23} b_{32}}$.

Here $P_i, Q_i;\ i = 1, 2, 3$ are constants that depend on Ω. $J_{1/2}$ and $Y_{1/2}$ are modified Bessel functions of order $\left(\dfrac{1}{2}\right)$ with First and Second kinds respectively. Resolving cubical dilation $(\overline{e})$ from equation (3.27) for displacement $\overline{U}$, we obtain

$$\overline{U} = x^{-\frac{1}{2}} \sum_{i=1}^{3} \frac{1}{k_i} R_i \left(P_i J_{3/2}(k_i x) - Q_i Y_{3/2}(k_i x) \right). \tag{3.29}$$

On differentiating equation (3.26) with respect to x, the temperature gradient is obtained as

$$\overline{\theta}_{,x} = x^{-\frac{1}{2}} \sum_{i=1}^{3} k_i \left[P_i J_{3/2}(k_i x) - Q_i Y_{3/2}(k_i x) \right], \tag{3.30}$$

Substituting the values of $\overline{e}, \overline{U}, \overline{\phi}, \overline{\theta}$ from equations (3.26–3.29) in equation (3.18) we get

$$\tau_{xx} = x^{-\frac{1}{2}} \sum_{i=1}^{3} \begin{pmatrix} P_i \left\{ \mathrm{H}_i J_{1/2}(k_i x) + 2\left(\dfrac{c_0 - 1}{k_i x} \right) R_i J_{3/2}(k_i x) \right\} \\ + Q_i \left\{ \mathrm{H}_i Y_{1/2}(k_i x) - 2\left(\dfrac{c_0 - 1}{k_i x} \right) R_i Y_{3/2}(k_i x) \right\} \end{pmatrix}, \tag{3.31}$$

$$\tau_{\theta\theta} = x^{-\frac{1}{2}} \sum_{i=1}^{3} \begin{pmatrix} P_i \left\{ \mathrm{H}_i^* J_{1/2}(k_i x) - \left(\dfrac{c_0 - 1}{k_i x} \right) R_i J_{3/2}(k_i x) \right\} \\ +Q_i \left\{ \mathrm{H}_i^* Y_{1/2}(k_i x) + \left(\dfrac{c_0 - 1}{k_i x} \right) R_i Y_{3/2}(k_i x) \right\} \end{pmatrix}, \tag{3.32}$$

where $\mathrm{H}_i = R_i + \bar{b}^* S_i - \bar{\beta}_R,\ \mathrm{H}_i^* = c_0 R_i + \bar{b}^* S_i - \bar{\beta}_R,\quad i = 1, 2, 3$.

3.5 Frequency relations

The frequency relations have been obtained by substituting the equations (3.26) to (3.31) for boundary conditions given in equations (3.8) and (3.9), for thermoelastic transversely isotropic hollow sphere with voids material for DPL model, when elastic material is considered as nonlocal and local under the impact of magnetic field at $x = 1$ and $x = \eta$ as inner and outer radii of the sphere. On simplification, we obtained following system of linear homogeneous equations:

$$\mathrm{M}\,\mathrm{X} = 0, \tag{3.33}$$

where $\mathrm{M} = (m_{ij})_{6\times 6};\ i, j = 1\,to\,6$ and $\mathrm{X} = (P_1, P_2, P_3, Q_1, Q_2, Q_3)^T$. The set of equations have been obtained from a non-trivial solution if the determinant of coefficient matrix M diminishes, hence frequency equations are given as:

$$\left| m_{ij} \right| = 0\ ;\quad i, j = 1\,to\ 6, \tag{3.34}$$

where, m_{ij} ; $i, j = 1\,to\ 6$ have been classified in thermally insulated/isothermal boundaries given below in separate sets I and II:

Set I: The constant elements of m_{ij} ; $i, j = 1\,to\ 6$ for equation (3.34)-are

$$\left. \begin{array}{r} m_{1j} = \mathrm{H}_i J_{1/2}(k_i) + 2\left((c_0 - 1)/k_i\right) R_i J_{3/2}(k_i), m_{3j} = S_i J_{1/2}(k_i),\ m_{5j} = k_i J_{3/2}(k_i) \\ ; i, j = 1,2,3 \\ m_{1j} = \mathrm{H}_i Y_{1/2}(k_i) - 2\left((c_0 - 1)/k_i\right) R_i Y_{3/2}(k_i), m_{3j} = S_i Y_{1/2}(k_i), m_{5j} = -k_i Y_{3/2}(k_i) \\ ; i = 1,2,3;\ j = 4,5,6 \end{array} \right\}, \tag{3.35}$$

Set II: Here in this set, the elements of $m_{1j}, m_{2j}, m_{3j}, m_{4j}$; $j = 1\ to 6$ remains same as given in equation (3.35). The remaining elements of m_{5j}, m_{6j} ; $j = 1\ to\ 6$ from the frequency equation (3.34) are:

$$m_{5j} = J_{1/2}\left(k_i\right);\ i, j = 1, 2, 3,\ \ m_{5j} = Y_{1/2}\left(k_i\right);\ i = 1, 2, 3;\ j = 4, 5, 6;\}. \quad (3.36)$$

Inserting η along with k_i, in m_{1j}, m_{3j}, m_{5j}; $j = 1\ to\, 6$ we obtain the constant elements of m_{2j}, m_{4j}, m_{6j}; $j = 1\ to\ 6$.

3.6 Deduction of analytical results

3.6.1 Generalized transversely isotropic magneto-thermoelastic hollow sphere with voids

If the nonlocal elastic parameter i.e. $\zeta_0 = 0$ has been ignored, then the above model reduces to DPL model of thermoelastic magneto sphere with voids**.**

3.6.2 Classical transversely isotropic thermoelastic hollow sphere

If nonlocal parameter, phase lag relaxation time parameters and voids constants have been ignored, i.e. $\zeta_0 = 0$, $\alpha = b = M = \xi_1 = \xi_2 = 0$ and $t_p = t_q = 0$ and system is in thermal equilibrium then the analysis of free vibrations is reduced to the coupled magneto-thermoelastic hollow sphere. Further if nonlocal, voids, magneto parameters, the phase-lags of temperature gradient relaxation time parameter are ignored i.e. $\zeta_0 = 0$, $\alpha = b = M = \xi_1 = \xi_2 = \phi = 0$, $\mu_e = H_0 = 0$, $t_p = 0$ and the value of heat flux is considered as $t_q = t_0$, $t_q^2 = 0$, also the functionally graded parameter $\alpha = 0$ has been taken from Sharma and Mishra (2017), then the governing equations in present chapter and Sharma and Mishra (2017) have been reduced to

$$\frac{\partial^2 u}{\partial x^2} + \frac{2}{x}\frac{\partial u}{\partial x} - \frac{2u}{x^2} - \bar{\beta}_R \frac{\partial \theta}{\partial x} = \frac{\partial^2 u}{\partial \tau^2}, \quad (3.37)$$

$$\frac{\partial^2 \theta}{\partial x^2} + \frac{2}{x}\frac{\partial \theta}{\partial x} - \Omega^*\left(\frac{\partial}{\partial \tau} + \tau_0 \frac{\partial^2}{\partial \tau^2}\right)\theta = \frac{\varepsilon_T \Omega^*}{\bar{\beta}_R}\left(\frac{\partial}{\partial \tau} + \tau_0 \frac{\partial^2}{\partial \tau^2}\right)\left(\frac{\partial u}{\partial x} + \frac{2}{x}u\right). \quad (3.38)$$

Hence the governing equations and the analysis have been reduced to transversely isotropic thermoelastic hollow sphere with LS model of generalized thermoelasticity which is good agreement with Sharma and Mishra (2017) without inhomogeneity parameter.

3.6.3 Elastic sphere

If the constants i.e. the nonlocal, voids, magneto, relaxation time parameters and thermo-mechanical constants are considered to be absent i.e. $\zeta_0 = 0$, $\alpha = b = M = \xi_1 = \xi_2 = \phi = 0$, $\mu_e = H_0 = 0$, $t_p = t_q = 0$ and $\beta_R = \varepsilon_T = T = 0$, also the functionally graded parameter $\beta = 0$ has been taken in Kele and Tutuncu (2011), then the governing equations of present chapter and Kele and Tutuncu (2011) are reduced to

$$\frac{\partial^2 u}{\partial x^2} + \frac{2}{x}\frac{\partial u}{\partial x} - \frac{2u}{x^2} = \frac{\partial^2 u}{\partial \tau^2}. \tag{3.39}$$

Therefore, the governing equations and free vibration analysis is reduced to transversally isotropic elastic sphere which is good agreement with Kele and Tutuncu (2011) in the absence of functionally graded materials.

3.7 Numerical results and discussion

Here in this section, for numerical simulations and computations, the analytical results in a transversely isotropic DPL model of generalized magneto nonlocal thermoelastic hollow sphere with voids material has been presented in this chapter. The numerical results has been performed for LS model, DPL model, CTE model and elasticity (E) in the absence and presence of magnetic fields at $\eta = 1.5,\ 2.0$. Modeling has been prepared for transversely isotropic thermoelastic solid with voids material single crystal of zinc whose physical constant values are given in SI units (Chadwick and Seet (1970))

$K_\theta = 1.24\times10^2 Wm^{-1}\deg^{-1}$, $c_{12} = 1.562\times10^{11}\ Nm^{-2}$, $c_{11} = 1.628\times10^{11}\ Nm^{-2}, T_0 = 296K$, $\beta_r = \beta_\theta = 5.75\times10^6\ Nm^{-2}\ \deg^{-1}, C_e = 3.9\times10^2\ JKg^{-1}\deg^{-1}$, $\rho = 7.14\times10^3 Kg\, m^{-3}, \omega = 10$.
And voids parameters are:

$\chi = 1.753\times10^{-15} m^2$, $\alpha = 3.688\times10^{-5} N, M = 2.0\times10^6 Nm^{-2}\deg^{-2}$,
$\xi_1 = \xi_2 = 1.475\times10^{10} Nm^{-2}$, $b = 1.13849\times10^{10} Nm^{-2}$

The parameters of magnetic fields are assumed as $\mu_e = 4\pi\times10^7 H/m$, $H_0 = 10^8\ A/m$ from Othman and Hilal (2017). The dual phase-lag parameters have been assumed as $t_p = 0.05$, $t_q = 0.07$ (Mondal (2019). The nonlocal parameter has been considered as $\xi_0 = 2.3102$ in Bachher and Sarkar (2019). The secular dispersion relations obtained using boundary conditions are transcendental equations, which are complex numbers (real as well as imaginary part) because of dissipative term in heat condition equation (3.4). The numerical simulations/computations have been employed to equation (3.34) for assumed thermally insulated boundary conditions.

The numerical Iteration method has been applied to evaluate the roots of equation (3.34), which is of the type $g(\Omega)=0$. The required substitution for the considered method is $\Omega=\Phi(\Omega)$, therefore, the sequence (Ω_n) of iterations has been generated for desired accuracy level. If the condition $\left|\Phi'(\Omega)\right| \ll 1,$ for all $\Omega \in I$, then the root of approximations will converge to $\Omega=\Omega_a$, provided $\Omega_0 \in I$, where I is the anticipated root of the interval. The numerical convergence i.e. $\left|\Omega_{n+1}-\Omega_n\right|<\varepsilon$, is the required condition for computations. Here ε has been chosen small arbitrary number to accomplish the required accuracy level selected randomly, which might be satisfied. Therefore, the above procedure is repeated continuously for the values of Ω (real as well imaginary part) many times until we obtain desired level of accuracy. The numerically analyzed complex values of Ω are formulated as $\Omega^m=\Omega_R^m+i\Omega_I^m$. Here the real part has been presumed as natural frequency $\Omega_R^m=\Omega_R$ and imaginary part as dissipation factor $\Omega_I^m=\Omega_I$ respectively. The mode number is denoted as parameter m , which corresponds to root of the transcendental equation. Hence, numerically analyzed natural frequencies have been presented graphically for the theories of thermoelasticity i.e. DPL, LS, CTE and E, for nonlocal and local thermoelastic hollow sphere under the impact of magnetic field (presence and absence). Variation of vibrations in nonlocal/local thermoelastic sphere has been shown graphically for of natural frequencies (Ω_R) versus mode number (m) with and without magnetic field at $\eta=1.5$ in Fig. 3.2 to Fig. 3.3. It is observed from Fig. 3.2 and Fig. 3.3 that initially the vibrations noted to have low trends but increases with increasing values of m . The behaviors of vibrations are higher in the absence of magnetic field in contrast to the presence of magnetic field for local and nonlocal elastic materials. This is noticed from Fig. 3.2 and Fig. 3.3 that the behavior of variations of real part (Ω_R) is larger for DPL model in comparison with LS, CTE and Elasticity models.

Moosapour et al. (2014) defined fractions of lost energy per cycle of vibrations as defined $Q=\sqrt{\left((\mathrm{Re}(\Omega_R^m)^2+\mathrm{Im}(\Omega_I^m)^2)\right)}/2\left|\mathrm{Im}(\Omega_I^m)\right|$. The number in denominator i.e. 2 has been occurred due to generated mechanical energy of the material, is relative to real part. This has been observed from computations that frequencies with real part are larger in comparison with imaginary part. Hence, thermoelastic damping is calculated as $Q^{-1}=2\left|\dfrac{\Omega_I}{\Omega_R}\right|$, from Sharma and Mishra (2017) for thermoelastic models. Here themoelastic damping Q^{-1} has been denoted as D_F. The fractional error $\varepsilon^{(Z^K)}$ from iterative computations in the real part of frequency Ω_R^m is defined as $\varepsilon^{(Z^K)}=\left(\mathrm{Re}(\Omega_R^m)^k-\mathrm{Re}(\Omega_R^m)^{k-1}\right)/\,\mathrm{Re}(\Omega_R^m)^{k-1}$ (Moosapour et al. (2014). Therefore, the error $\varepsilon^{(Z^*)}$ will go down below the accepted value, and the process of iteration ends. Hence, the frequency shift (Ω_{shift}) has been defined as $\Omega_{shift}=\left|\dfrac{(\Omega_R^{Z^*}-\Omega_R^E)}{\Omega_R^E}\right|$ (Sharma et al. (2022b)). Here Z^* stands for CTE, LS, DPL models and E is elasticity.

The Fig. 3.4 represents frequency shift (Ω_{shift}) versus mode number (m) for LS, CTE and DPL at normalized thickness $\eta=1.5$ for nonlocal elastic sphere with voids in presence and absence of magnetic field. It has been seen from Fig. 3.4(a) (with magnetic field) that initially the variation of vibrations of frequency shift are lower, with increasing value of mode number the peak values have been noticed at $m=4.0$, and at the value of $m=5.0$, the variations become linear.

Fig. 3.4(b) (without magnetic field) depicts that initially the variations are low, become maximum at $m=4.0$ and the variation of vibrations decreases with increasing values of mode number. Frequency shift against mode number for three different models LS, CTE and DPL at normalized thickness of the sphere/disk $\eta=1.5$ for local elasticity with voids in presence/absence of magnetic field has been shown in Fig.3.5. It has been revealed from Figs. 3.5(a) and 3.5(b) that in the beginning the behavior of vibrations is larger, decreases up to $m=3.0$ and from left to right vibrations decreases linearly. It has been observed from Figs. 3.4 and 3.5 that the frequency shift is larger in case of DPL model in comparison with LS and CTE models of thermoelasticity. Fig. 3.6 and Fig. 3.7 are presented for frequency shift (Ω_{shift}) against mode number (m) at LS, DPL, and CTE at radius $(\eta = 2.0)$ in magneto-thermoelastic voids sphere with and without magnetic field in nonlocal/local elastic materials.

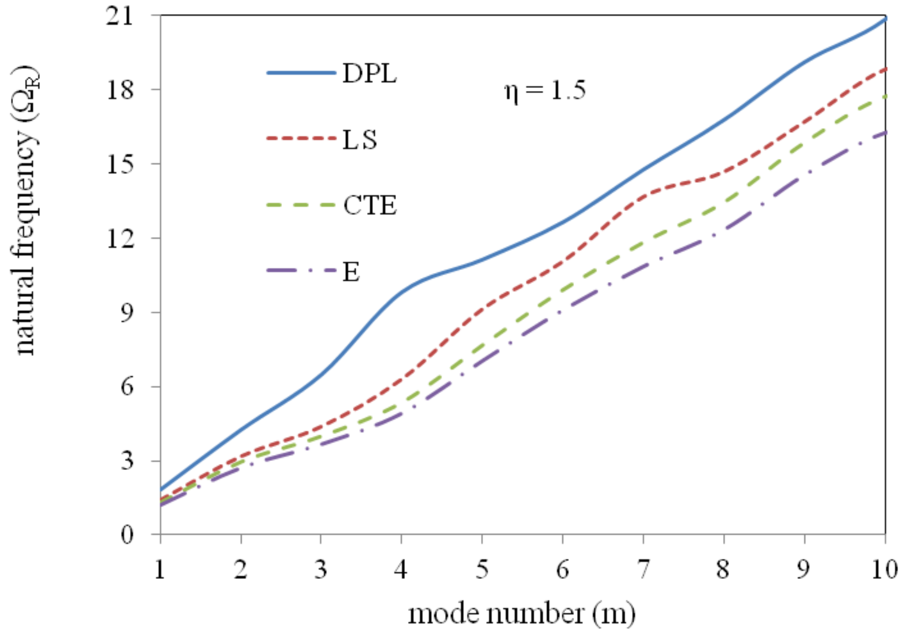

Figure 3.2(a): Variation of natural frequencies (Ω_R) against mode number (m) for thermoelastic models at $\eta = 1.5$ in nonlocal case with magnetic field.

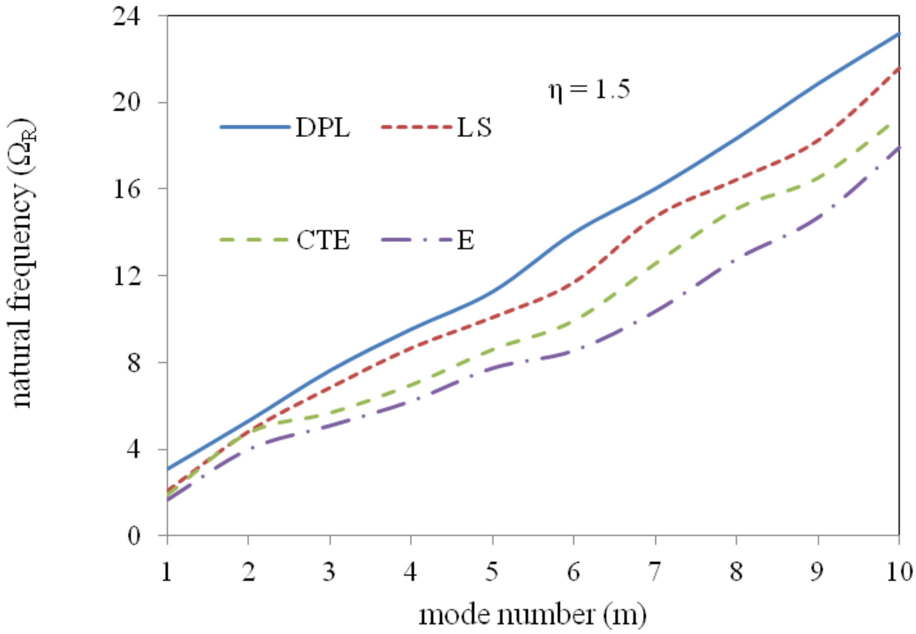

Figure 3.2(b): Variation of natural frequencies (Ω_R) against mode number (m) for thermoelastic models at $\eta = 1.5$ in nonlocal case without magnetic field.

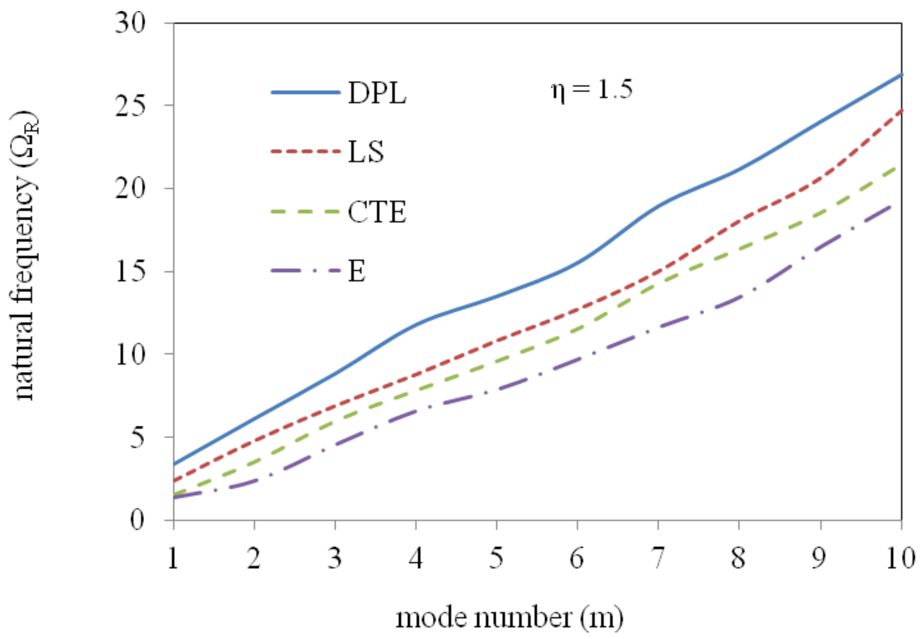

Figure 3.3(a): Variation of natural frequencies (Ω_R) against mode number (m) for thermoelastic models at $\eta = 1.5$ in local case with magnetic field.

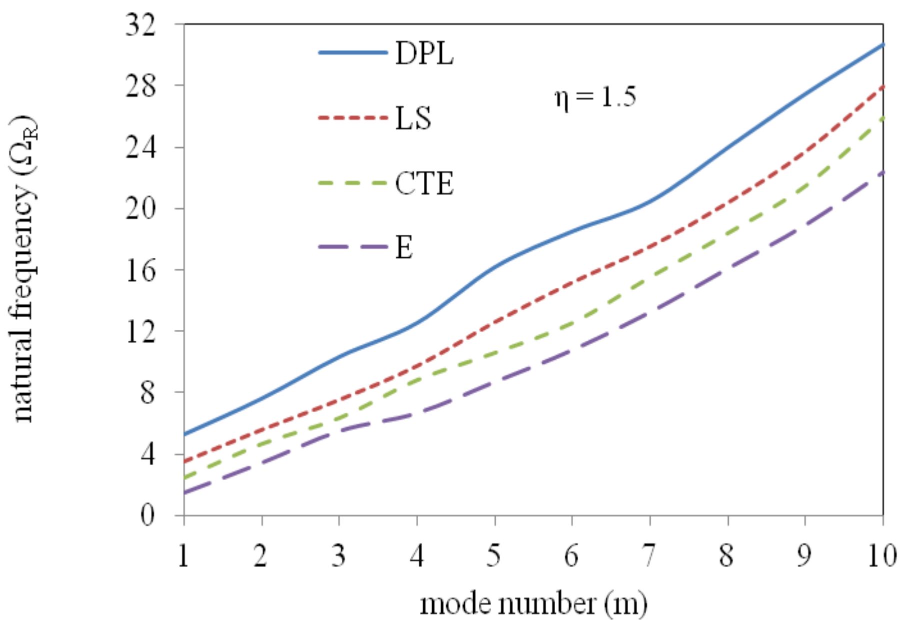

Figure 3.3(b): Variation of natural frequencies (Ω_R) against mode number (m) for thermoelastic models $\eta = 1.5$ in local case without magnetic field.

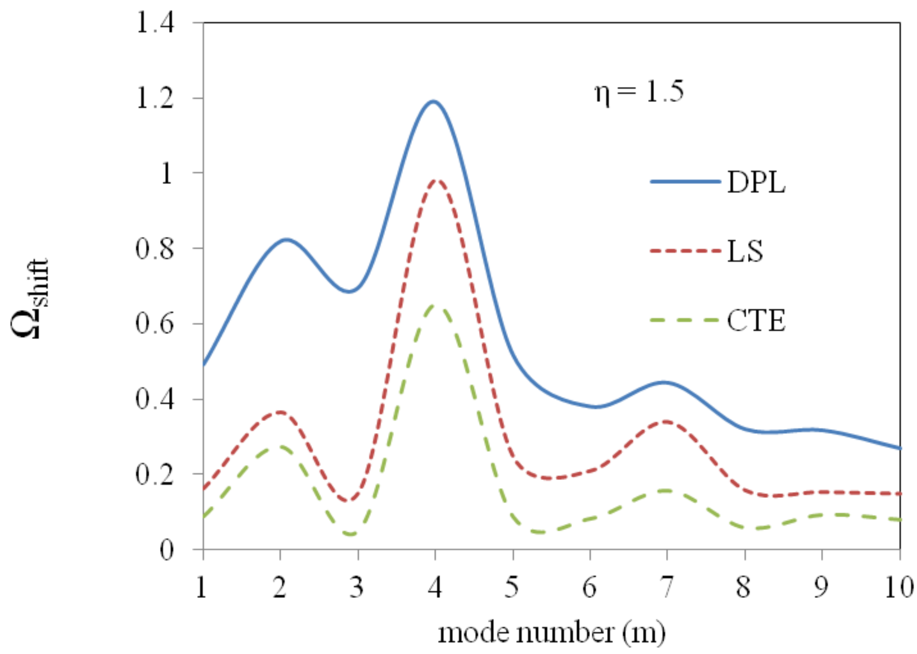

Figure 3.4(a): Variation of frequency shift (Ω_{Shift}) against mode number (m) for thermoelastic models at $\eta = 1.5$ in nonlocal case with magnetic field.

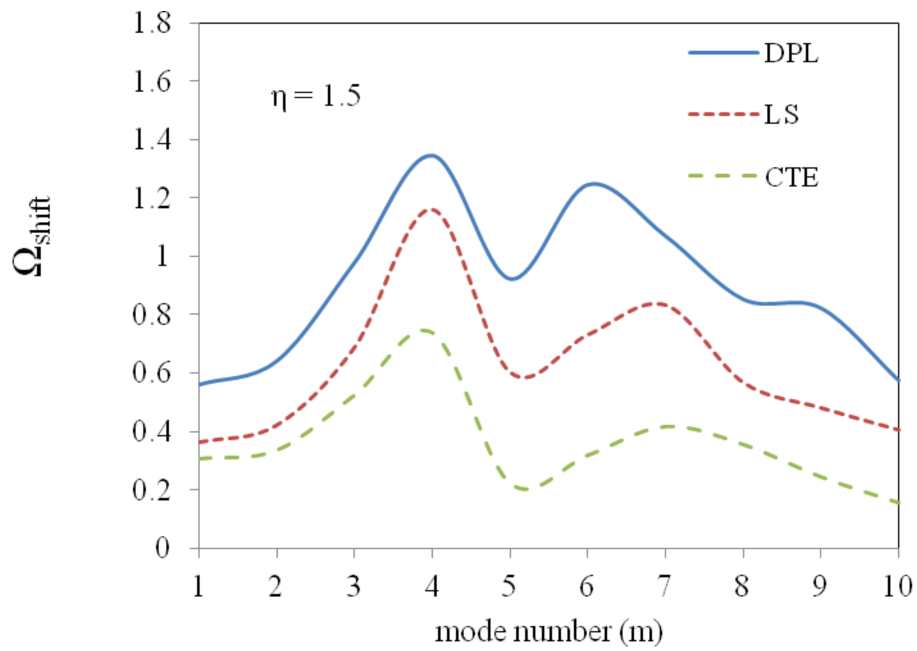

Figure 3.4(b): Variation of frequency shift (Ω_{Shift}) against mode number (m) for thermoelastic models at $\eta = 1.5$ in nonlocal case without magnetic field.

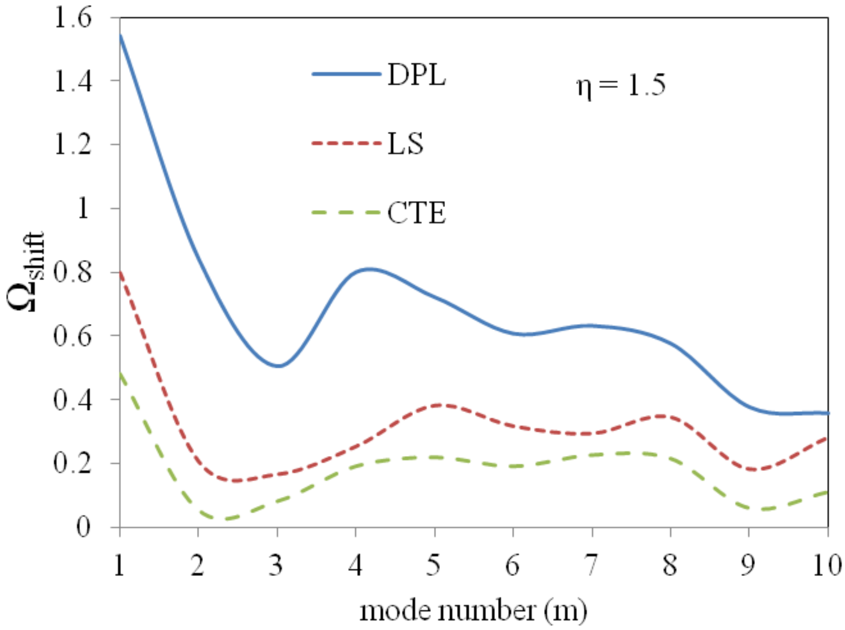

Figure 3.5(a): Variation of frequency shift (Ω_{Shift}) against mode number (m) for thermoelastic models at $\eta = 1.5$ in local case with magnetic field.

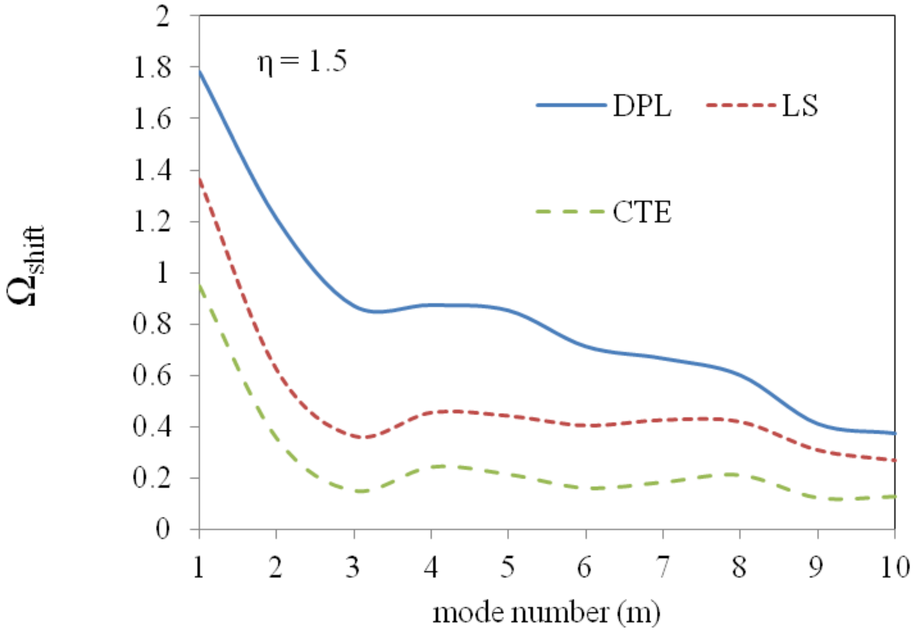

Figure 3.5(b): Variation of frequency shift (Ω_{Shift}) against mode number (m) for thermoelastic models at $\eta = 1.5$ in local case without magnetic field.

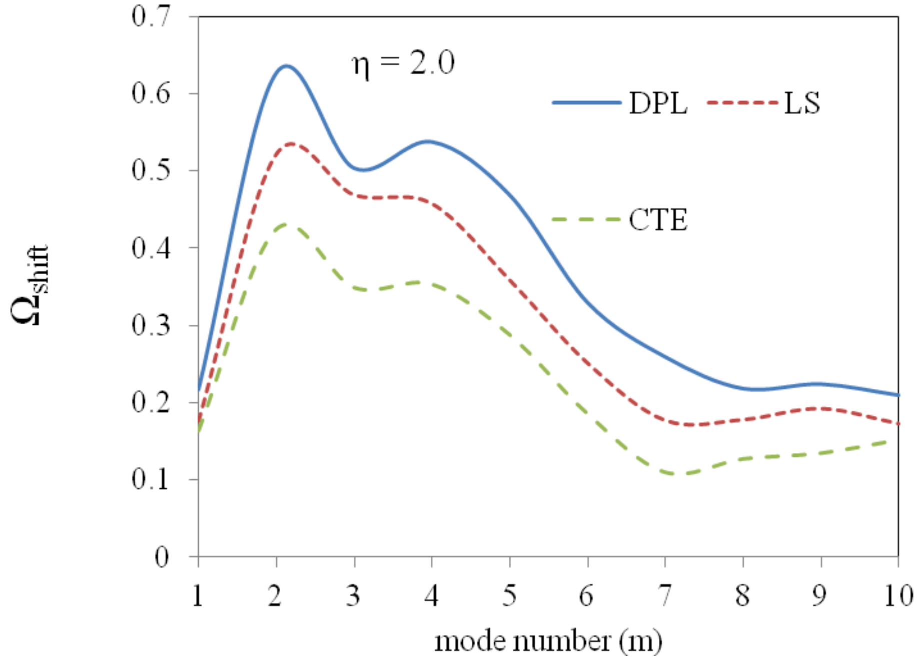

Figure 3.6(a): Variation of frequency shift (Ω_{Shift}) against mode number (m) for thermoelastic models at $\eta = 2.0$ in nonlocal case with magnetic field.

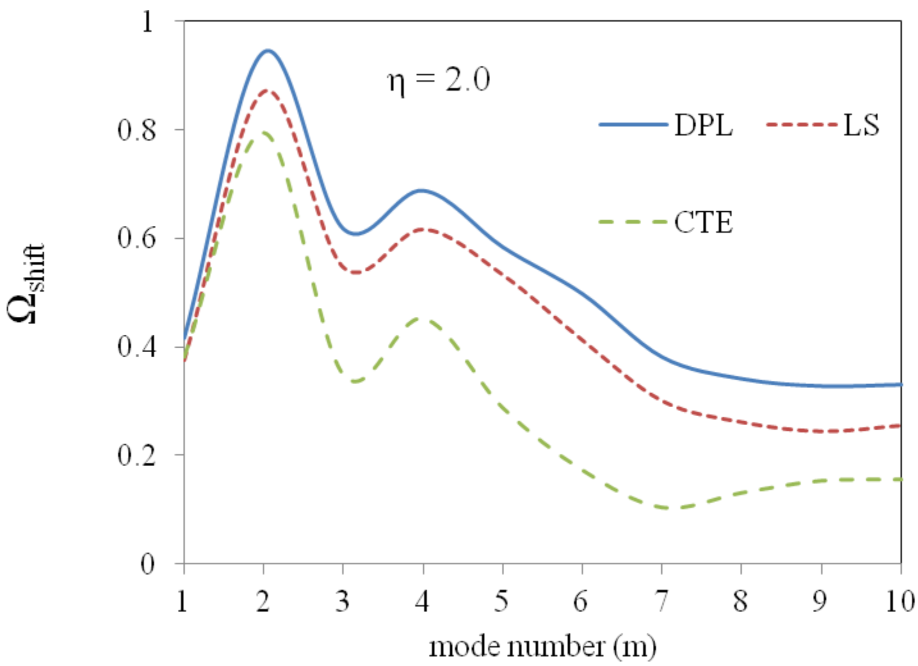

Figure 3.6(b): Variation of frequency shift (Ω_{Shift}) against mode number (m) for thermoelastic models at $\eta = 2.0$ in nonlocal case without magnetic field.

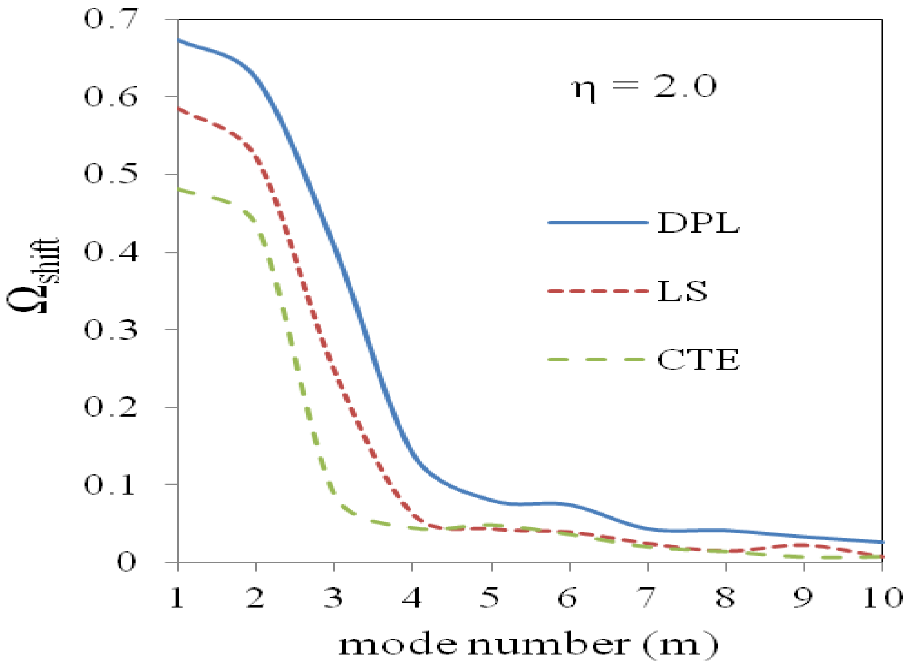

Figure 3.7(a): Variation of frequency shift (Ω_{Shift}) against mode number (m) for thermoelastic models at $\eta = 2.0$ in local case with magnetic field.

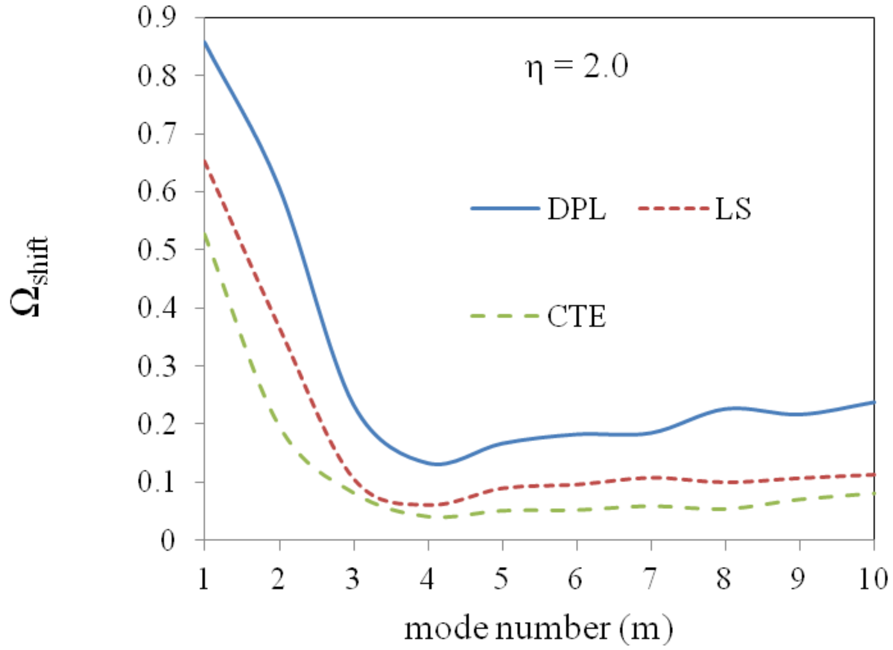

Figure 3.7(b): Variation of frequency shift (Ω_{Shift}) against mode number (m) for thermoelastic models at $\eta = 2.0$ in local case without magnetic field.

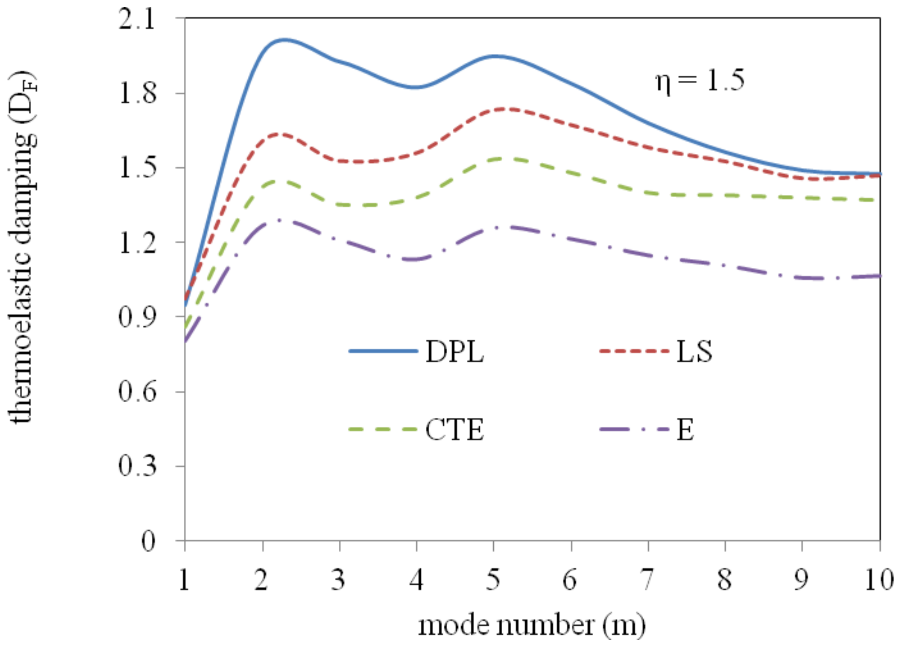

Figure 3.8(a): Variation of thermoelastic damping (D_F) against mode number (m) for thermoelastic models at $\eta = 1.5$ in nonlocal case with magnetic field.

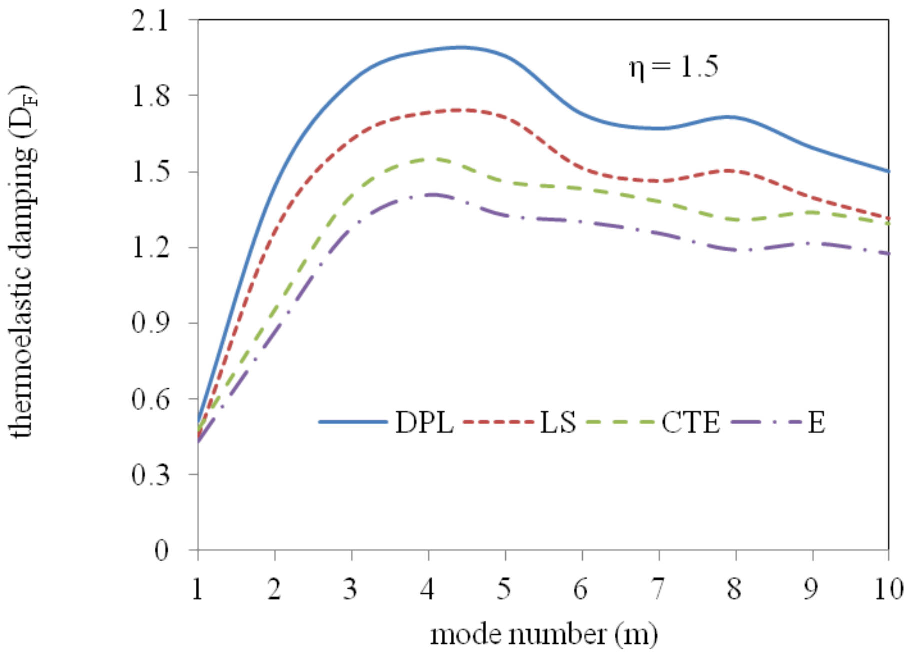

Figure 3.8(b): Variation of thermoelastic damping (D_F) against mode number (m) for thermoelastic models at $\eta = 1.5$ in nonlocal case without magnetic field.

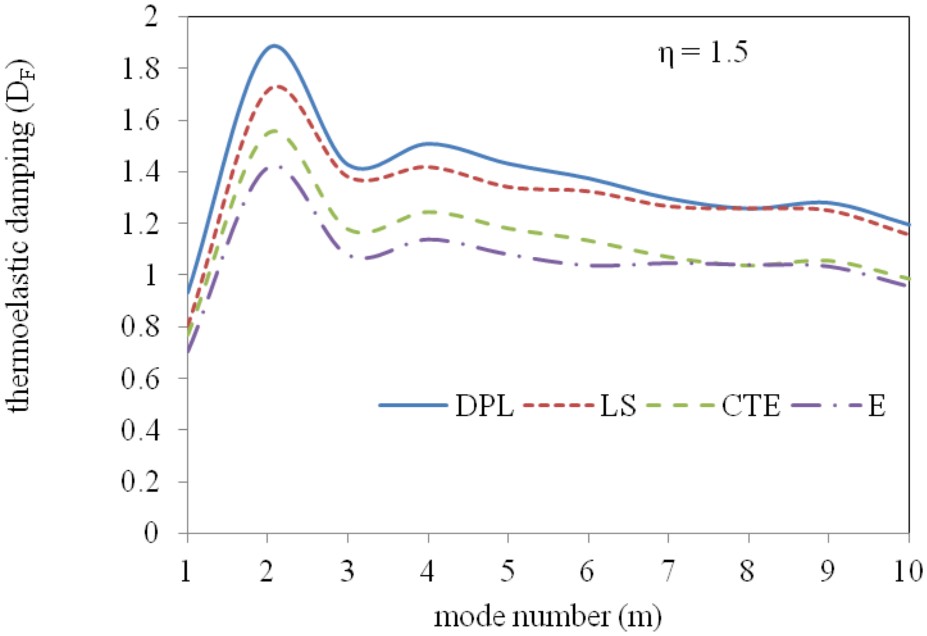

Figure 3.9(a): Variation of thermoelastic damping (D_F) against mode number (m) for thermoelastic models at $\eta = 1.5$ in local case with magnetic field.

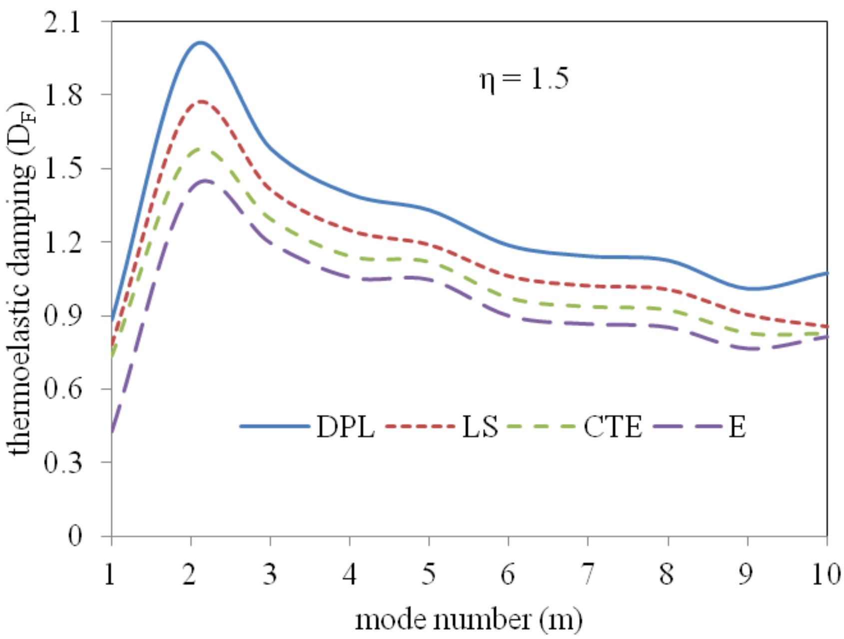

Figure 3.9(b): Variation of thermoelastic damping (D_F) against mode number (m) for thermoelastic models at $\eta = 1.5$ in local case without magnetic field.

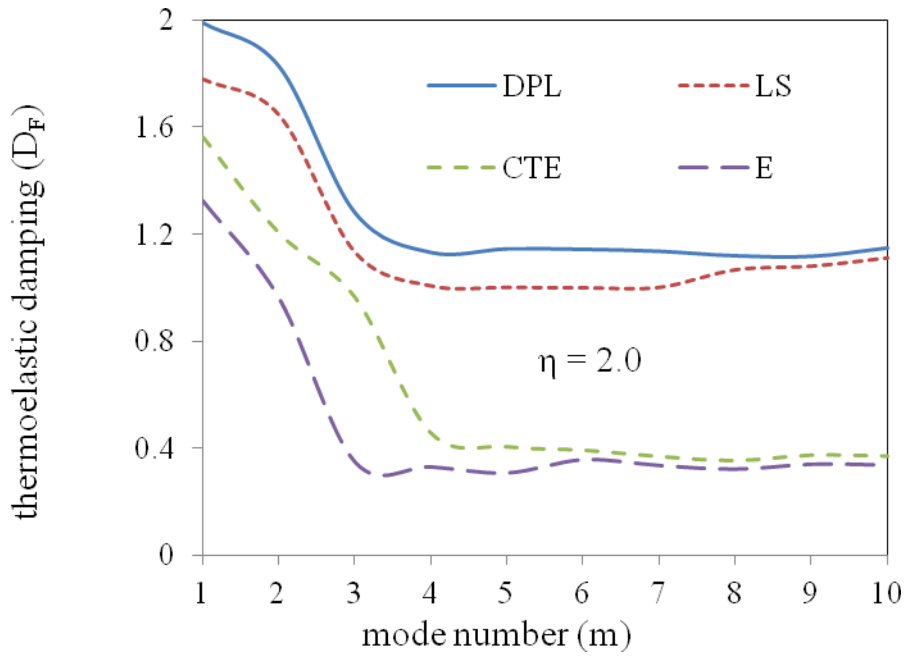

Figure 3.10(a): Variation of thermoelastic damping (D_F) against mode number (m) for thermoelastic models at $\eta = 2.0$ in nonlocal case with magnetic field.

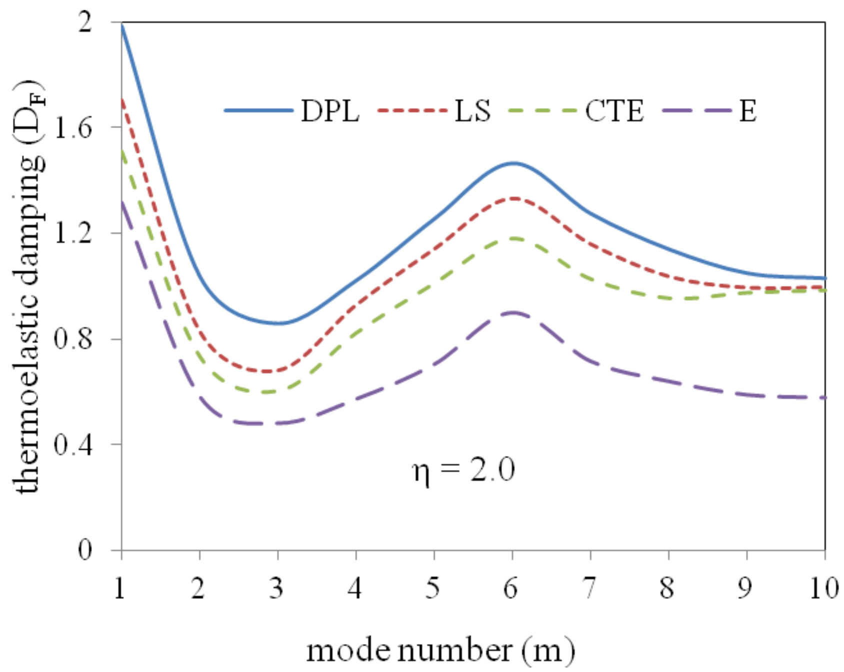

Figure 3.10(b): Variation of thermoelastic damping (D_F) against mode number (m) for thermoelastic models at $\eta = 2.0$ in nonlocal case without magnetic field.

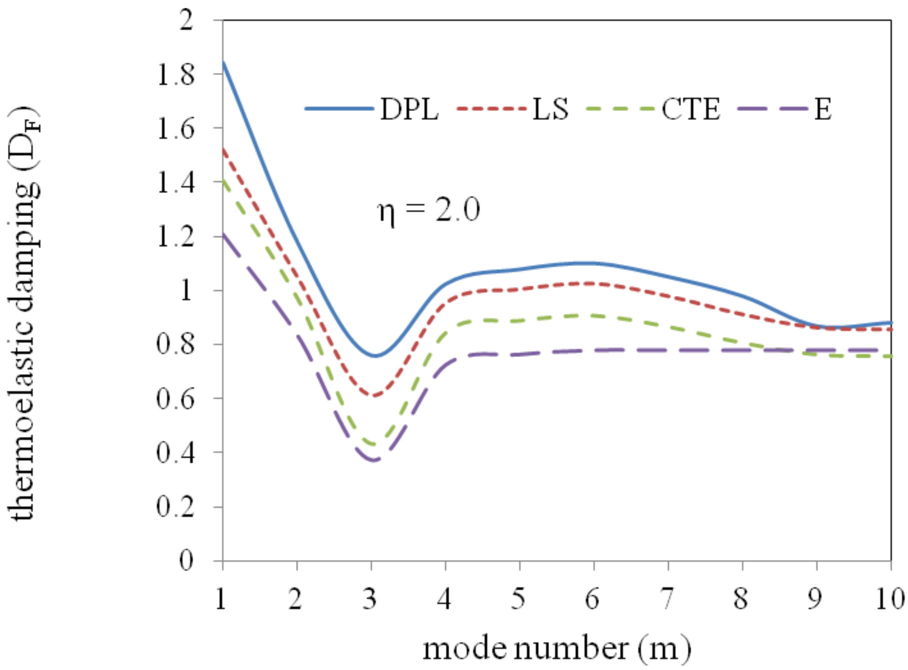

Figure 3.11(a): Variation of thermoelastic damping (D_F) against mode number (m) for thermoelastic models at $\eta = 2.0$ in local case with magnetic field.

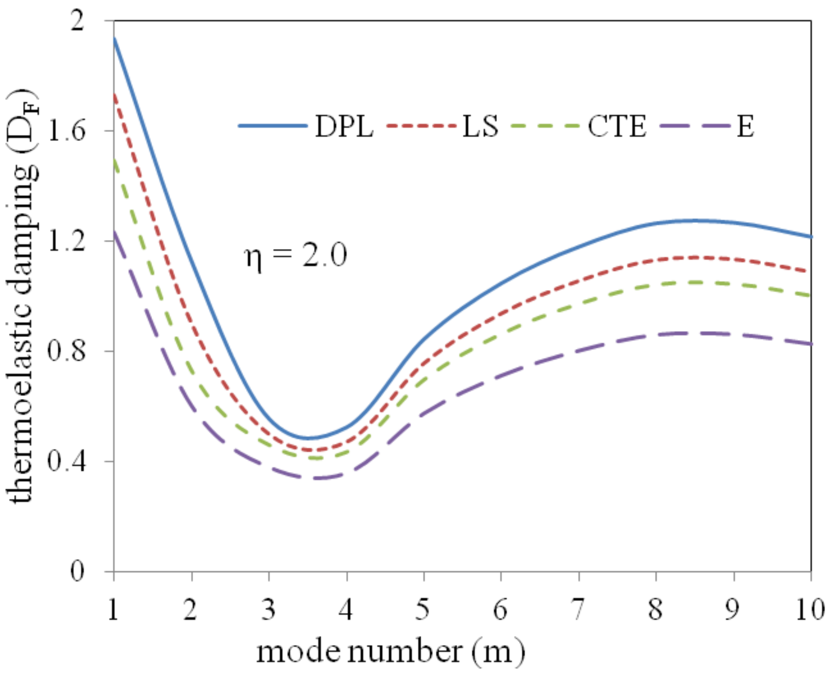

Figure 3.11(b): Variation of thermoelastic damping (D_F) against mode number (m) for thermoelastic models at $\eta = 2.0$ in local case without magnetic field.

It is revealed from Fig. 3.6(a) that Ω_{shift} vibrations are low in beginning, increases up to $m = 2.0$, then vibrations go on decreasing to become linear at $m = 6.0$. Fig. 3.6(b) shows meager vibrations initially, achieve maximum amplitude at $m = 2.0$, then it shows small dip values at $m = 3.0$ and decreases linearly as mode number increases. From Fig. 3.7 we observe that initial trends in the vibrations are larger, go on decreasing up to $m = 4.0$ and become linear with increasing values of m.

Figs. 3.8, 3.9, 3.10 and 3.11 have been shown for nonlocal and local elastic spheres with voids for thermoelastic damping (D_F) against mode number (m) in presence/absence of magnetic field, in DPL, CTE, LS and E at $\eta = 1.5$ and $\eta = 2.0$ respectively. Fig. 3.8(a–b) (nonlocal case at $\eta = 1.5$) revealed that initially the variation is low, achieve the maximum amplitude between $2.0 \le m \le 4.0$, then decreases linearly. It has been noticed from Fig. 3.9(a–b) (local case at $\eta = 1.5$) that initially the thermoelastic damping vibrations are low and peak value is noted at $m = 2.0$, then deceases linearly with increasing values of m. It has been concluded from Fig. 3.10(a) that initially the variation of thermoelastic damping vibrations is larger, decreases up to $m = 3.0$ and become linear with increasing values of m. Also, it is noticed from Fig. 3.10(a) (nonlocal case) that variations in DPL, LS are larger in contrast to CTE, elasticity (E) models. Fig. 3.10(b) for nonlocal case depicts that variation of D_F is larger initially, noted to be dip values between $2.0 \le m \le 0.3$, achieve maximum amplitude at $m = 6.0$ and decreases linearly after $m = 6.0$. It is revealed from Fig. 3.11(a) for local case that variation of thermoelastic damping vibrations is larger initially, decreases to achieve dip values between $2.0 \le m \le 3.0$, and go on increasing to become linear at $m = 6.0$. Fig. 3.11(b) for local case shows that initially variation of vibrations are larger, decreases to achieve dip for $2.0 \le m \le 5.0$, and increases linearly with m. All the figures depict that the variation of vibrations are larger in case of DPL model in comparison with LS, CTE and elasticity (E) cases of thermoelasticity. Also in some figures, due to the effect of magnetic field the behavior of vibrations is found to be larger without magnetic field in contrast to with magnetic field. It is also noted that thermoelastic damping variation of vibrations increases and decreases with increase in mode number due to coupling of elastic field in the mechanical, temperature field, voids volume fraction and magnetic fields.

3.8 Conclusions and Remedies

In this chapter, the analysis for electro-magneto transversely isotropic nonlocal generalized thermoelastic hollow sphere with voids, have been represented. Ordinary differential equations have been acquired from governing equations by applying time harmonics. The outer and inner surfaces of hollow sphere have been considered stress free, free from voids volume fraction and thermally insulated/isothermal conditions. From the calculated analytical and numerical results/discussions, following conclusions have been observed:

1. This is observed from all the figures that the variation of vibrations is larger for DPL model of generalized thermoelasticity in contrast to other models because of the effect of relaxation time parameter.
2. The effect of magnetic field clearly indicates that the variations are larger in absence of magnetic field in contrast to presence of magnetic field. The graphs representing natural frequencies clearly indicate that variation of vibrations go on increasing as the value of mode number increases.
3. The frequency equations have been derived and examined computationally for analytical results. The effect of DPL model of generalized magneto thermoelastic hollow sphere is represented numerically for field functions of free vibration analysis in presence/absence of magnetic field.
4. With increasing values of mode number, it is observed that the behavior of thermoelastic damping becomes linear after achieving maximum amplitude, because of the coupling between elastic, voids equilibrated volume fraction and thermal fields. The frequency shift, damping and natural frequencies are influenced by non-locality effect and represented for nonlocal and local cases with and without magnetic fields.
5. The results obtained in this chapter might prove useful applications for those who are active in research activities in seismology for drilling and mining in the earth’s crust. The study also finds applications for physicist/researchers who are working in the field of designing of new materials as well as in practical situations as in geomagnetic, optics, geophysics, acoustics, and oil prospecting etc.

6. The study of present chapter find applications in the field of science and engineering that the models like LS, DPL and CTE generalized thermoelasticity provide better and easier description to allow voids and relaxation time parameters. From current work, researchers receive the motivation to examine the free vibration analysis of conducting elastic, thermoelastic and magneto-thermoelastic materials with voids as novel applications in continuum mechanics.